Development and characterization of chlorine-selective pulsed discharge emission detector for gas chromatography

ARTICLE *in* JOURNAL OF CHROMATOGRAPHY A · APRIL 2000

Impact Factor: 4.17 · DOI: 10.1016/S0021-9673(99)01173-5 · Source: PubMed

3 AUTHORS, INCLUDING:

Stanley D Stearns
Valco Instruments (VICI)
44 PUBLICATIONS **401** CITATIONS

ELSEVIER

Journal of Chromatography A, 872 (2000) 141–165

JOURNAL OF CHROMATOGRAPHY A

www.elsevier.com/locate/chroma

Development and characterization of chlorine-selective pulsed discharge emission detector for gas chromatography

Kefu Sun[a], Wayne E. Wentworth[a,*], Stanley D. Stearns[b]

[a]*Department of Chemistry, University of Houston, 4800 Calhoun Road, Houston, TX 77204-5641, USA*
[b]*Valco Instruments Co., Inc., PO Box 55603, Houston, TX 77255, USA*

Received 24 June 1999; received in revised form 2 November 1999; accepted 4 November 1999

Abstract

A novel chlorine-selective pulsed discharge emission detector (Cl-PDED) for gas chromatography has been developed based on a reaction of krypton with chlorine and a unique design of the detector. A krypton ion produced in the krypton-doped helium pulsed discharge reacts with chlorinated compounds within the pulsed discharge to produce an excited species of KrCl* which emits at 221~222 nm. The reaction has the following advantages in respect to the detection of chlorinated compounds: (1) the reaction is an ion–molecule reaction that is 100–1000 times faster than a reaction of neutrals, which greatly enhances the sensitivity; (2) the KrCl* emission wavelength is far separated from interfering C emissions at 193. and 247.3 nm; (3) the KrCl* emission is transparent to air and can be recorded without a helium purge of the monochromator. The detector itself has been designed to have the following features: (1) the detector has a microvolume of the pulsed discharge region, ca. 0.35 μl, which increases the discharge power density to enhance the sensitivity; (2) this microvolume detector allows the use of a low flow-rate of ~5 ml/min, which enhances the sensitivity by the lower dilution of the column effluent; (3) the pulsed discharge is sufficiently narrow to replace the monochromator entrance slit, which gives much greater light gathering power; (4) the discharge electrodes are protected with a helium purge to prevent carbon deposition on the electrodes. This new Cl-PDED is the most sensitive chlorine-selective detector with a minimum detectability of ~50 fg Cl/s. The selectivity to carbon is 1000. There are no significant carbon emission lines in the KrCl* emission wavelength region, but the carbon continuum interference (stray light) limits the selectivity. The selectivity could be increased if a double monochromator were used to diminish the stray light. The detector linear range is over three orders of magnitude from 40 fg Cl to ~130 pg Cl, and the dynamic range is ~4 orders of magnitude. The relative standard deviation of the elemental response to chlorinated compounds is about 5%.

Keywords: Dectection, GC; Pulsed discharge emission detection; Chlorine selective detector; Krypton; Organochlorine compounds

1. Introduction

There are many applications, especially in environmental analyses, where there is a need for the analysis of chlorinated compounds. This can be a total chlorine analysis but more commonly the amount of the individual chlorinated compounds is analyzed. For the latter it is common to use a gas chromatographic separation of the mixture followed by a chlorine-selective detector, or a selective detector such as the electron capture detector. The chlorine-selective detector most commonly used for the

*Corresponding author.

0021-9673/00/$ – see front matter
PII: S0021-9673(99)01173-5

detection of chlorinated compounds is the electrolytic conductivity detector (ELCD). The ELCD is frequently referred to as the Hall detector, the name coming from the inventor (Randall C. Hall) who refined the detector for the selective detection of halogen, sulfur and nitrogen containing compounds [1–4]. In a text edited by Hill and McMinn [5], Chapter 6 is written by Hall on the use of commercially available ELCDs as detectors for capillary column chromatography. Since the focus of this study is on the chlorine-selective detection, the use of the ELCD as a chlorine detector only will be considered in this study. For the detection of chlorinated compounds with the ELCD, the column effluent is mixed with H_2 gas and reacted in a nickel tube which catalyzes the reaction at 850–1000°C to HCl. The reaction with aromatic chloro-compounds requires a higher temperature than the reaction with aliphatic chlorides due to the higher aromatic–Cl bond dissociation energy [5]. However, the nickel reaction tubes tend to lose their catalytic activity and need to be replaced periodically. The HCl produced from the reaction with H_2 is absorbed in propyl alcohol and its presence is detected quantitatively by a conductivity cell. The propyl alcohol must be pumped at a precise rate and continuously cleaned, if recycled, in order to maintain a constant baseline. Propyl alcohol is used since it selectively absorbs HCl and not the CH_4 produced from the carbon in the organic compounds. The conductivity cell is rather sensitive and the detection limit of Cl for the ELCD is quoted as ~1 pg/s. The response to Cl in the ELCD has a dynamic range of about five orders of magnitude, but the response is non-linear, especially at higher concentrations [5]. The ELCD operation requires catalyst tubes, solvents, resin cartridges, pumps and transfer lines. Compared to most GC detectors it is rather complicated and care must be exercised in order to obtain consistent results over long periods of time.

More recently a halogen selective detector [6–8] has been developed by OI Analytical (OI Analytical, College Station, TX, USA) which has the same sensitivity as the ELCD. The linear range of the response is quoted in its product specifications on Model 5360 (XSD) as 10^4. The principle behind the operation of the detector is an oxidative pyrolysis of the GC effluent over platinum heating coils to form halogen atoms from halogen-containing compounds. The halogen atoms then react with an alkali-sensitized cathodic surface, which yields an increased thermionic emission of free electrons and halide ions. Collection of these negative species comprises the signal in the form of a cathodic current.

In this study we describe a Cl-selective pulsed discharge emission detector (Cl-PDED) based upon the molecular emission from KrCl*. Low concentrations of Kr in helium (~0.1–0.4%) are sufficient to react with chlorinated compounds in the pulsed discharge emission detector to produce an excited state of KrCl* which emits in a fairly narrow molecular band at 221–222 nm. Since this emission is in the ultraviolet region, spectrometers with conventional quartz optics are sufficient to detect this emission. During the course of our studies with the PDED we observed the reaction of Cl-containing organic compounds with Kr quite by accident, but the formation of KrCl* is well documented in the literature [9–11] and is widely used in an ultraviolet laser which is commercially available. Like the chlorine–krypton reaction, we also observed the reaction of fluorine with krypton in the pulsed discharge emission detector at 248.5 nm [9–11], which could be used for the fluorine-selective detection.

In the development of this Cl-selective pulsed discharge detector based upon the formation of KrCl*, we have redesigned the detector to have a small internal volume of only ~0.35 μl. This reduction in volume allows the use of such low flow-rates as 3~5 ml/min. This not only makes the operation more economical but the lower dilution of the GC effluent with these low flow-rates enhances the sensitivity of the detector. The pulsed discharge in the Cl-PDED is also sufficiently narrow that the discharge can be used as the optical image, eliminating the entrance slit to the monochromator [12]. Elimination of the entrance slit gives much greater light gathering power into the spectrometer, which also is a major factor contributing to the higher sensitivity of this detector.

2. Experimental

Fig. 1 shows a block diagram of the entire

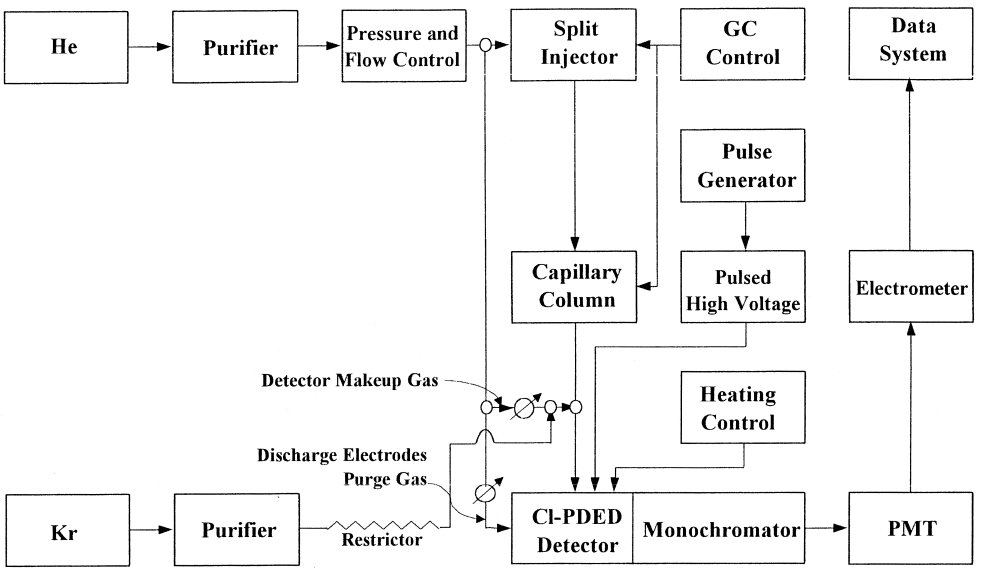

Fig. 1. Block diagram of the entire apparatus and flow configurations.

apparatus including the flow of the gases. The Kr-doped helium was made by mixing the pure krypton (99.999%, Air Liquide America, Houston, TX, USA) with the pure helium (99.999%, Air Liquide America). In order to obtain a small flow-rate of Kr-dopant gas, the Kr was passed through a fixed restrictor at a controlled pressure. The fixed restrictor was made by constricting a piece of 1/16 in. (1 in.=2.54 cm) stainless tubing with 0.01 in. I.D. The Kr concentration in Kr-doped helium can be adjusted by changing the regulator pressure of the Kr cylinder. The Kr flow-rate as a function of Kr pressure is shown in Fig. 2. The curve fits a power function of the Kr flow-rate versus the Kr pressure with a coefficient of determination $R^2=0.994$. Valco gas purifiers (Valco, Houston, TX, USA) were used on both the He and Kr gases. The purity of chemicals used in this study was above 99%.

Details of the Cl-PDED, spectrometer, gas chromatograph, chromatographic data system and pulse generator in Fig. 1 will be discussed in the following sections.

2.1. Chlorine-selective pulsed discharge emission detector

Since the Cl-PDED utilizes the UV emission at 221~222 nm from KrCl*, a quartz window can be used without any serious diminution of the emission intensity. A schematic diagram of the entire Cl-PDED including the spectrometer is shown in Fig. 3. The detector position is actually perpendicular to that shown in Fig. 3 so that the discharge is co-linear with the entrance slit normally used in the monochromator. Likewise the PMT is perpendicular to that shown in Fig. 3 so that the axis of the cylindrical photomultiplier tube (PMT) is co-linear with the exit slit. The Cl-PDED was attached directly to the entrance of the monochromator. Fig. 4 shows the

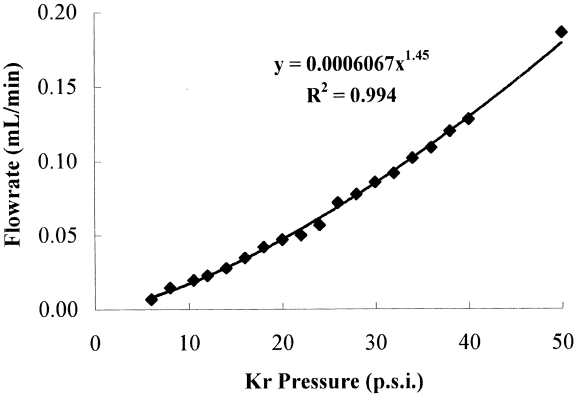

Fig. 2. Krypton flow-rate versus pressure (1 p.s.i.=6894.76 Pa).

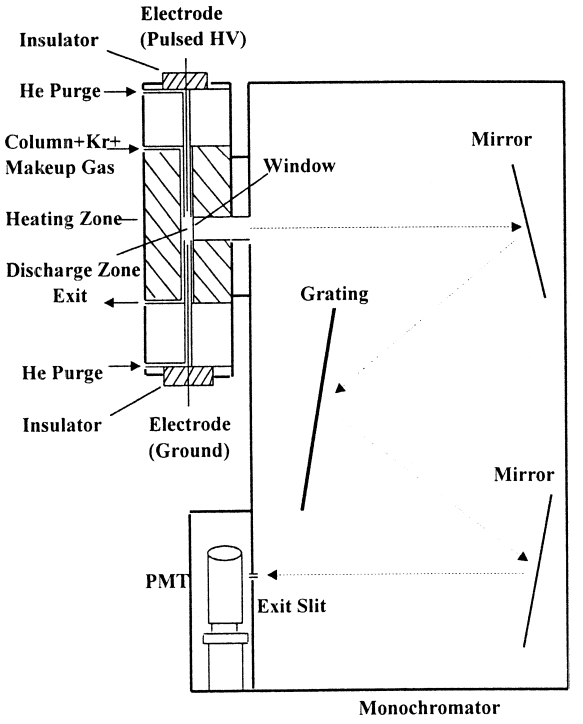

Fig. 3. Schematic diagram of Cl-PDED and spectrometer. Detector and PMT are rotated 90°C out-of-plane in order to show the cross sectional view.

detailed structure of the Cl-PDED. The Cl-PDED consists of concentric fused-silica tubing where the column effluent is introduced through the Tee at the inlet of the Cl-PDED and passes between the outside tubing and the next inner tubing which contains the Mo electrode. The outside tubing was a piece of uncoated fused-silica megabore column (0.53 mm I.D.×0.67 mm O.D.) with the polyimide coating burned off in the discharge region to allow transmission of the UV radiation through the fused-silica. The inner uncoated fused-silica tubing containing the Mo electrode had an I.D. of 0.32 mm and an O.D. of 0.43 mm. The outside tubing was mounted in a 1/4 in. stainless steel Tee and the distance from the monochromator wall was adjusted so that the discharge coincided with the optical image of the monochromator, which is usually defined by the entrance slit. The reason for this is to enhance the light gathering from the discharge, thus giving a higher sensitivity for the analysis. This is similar to the design discussed in another paper [12].

The 0.43 mm O.D. fused-silica tubing was mounted in a special 1/16 in. Tee consisting of a male fitting at one end and a female fitting at the other end. The 1/16 in. stainless steel tubing coming from the side was silver-soldered into the body of the Tee. The Tee was made so that the internal volume was kept to a minimum.

The 1/4 in. Tee was heated by a heating collar conventionally used for this purpose. The 1/4 in. cartridge heater supplied the heat to the collar and was controlled by a Valco temperature controller. A hole was drilled perpendicular to the face of the Tee in order to allow the emission to enter the spectrometer.

The volume of the discharge region is so small, ca. 0.35 μl, that lower gas flow-rates of 3~5 ml/min for the Cl-PDED could be used, thus increasing the concentration of the analyte and increasing the sensitivity of the analysis. Furthermore, lower flow-rates will allow the use of smaller helium cylinders and make the portability of the detector more feasible. Also a smaller detector volume will make the detector more amenable to high speed chromatography where very narrow peak widths are obtained.

Note that the electrodes are purged by the flow of the helium inside the tubing surrounding the metal electrode to prevent carbon deposition on the electrodes and to keep the electrodes at a relatively low temperature by removing the heat generated by the discharge. A flow of ~1 ml/min was used for this purpose and seemed to be satisfactory since no carbon deposits were observed on the metal electrodes, and there was no significant carbon emission at 193.1 nm when the detector was free of analyte. The metal electrode was a piece of 0.25 mm diameter molybdenum wire (99.95%, Aldrich, Milwaukee, WI, USA). There was some deterioration of the electrode over a period of a few months. In a future design a larger diameter Mo wire, probably 0.50 mm diameter, will be used to prevent or diminish the rate of deterioration. Also the detector can be so designed that the electrodes are easily replaced.

2.2. Spectrometer

For the most part of this study the monochromator

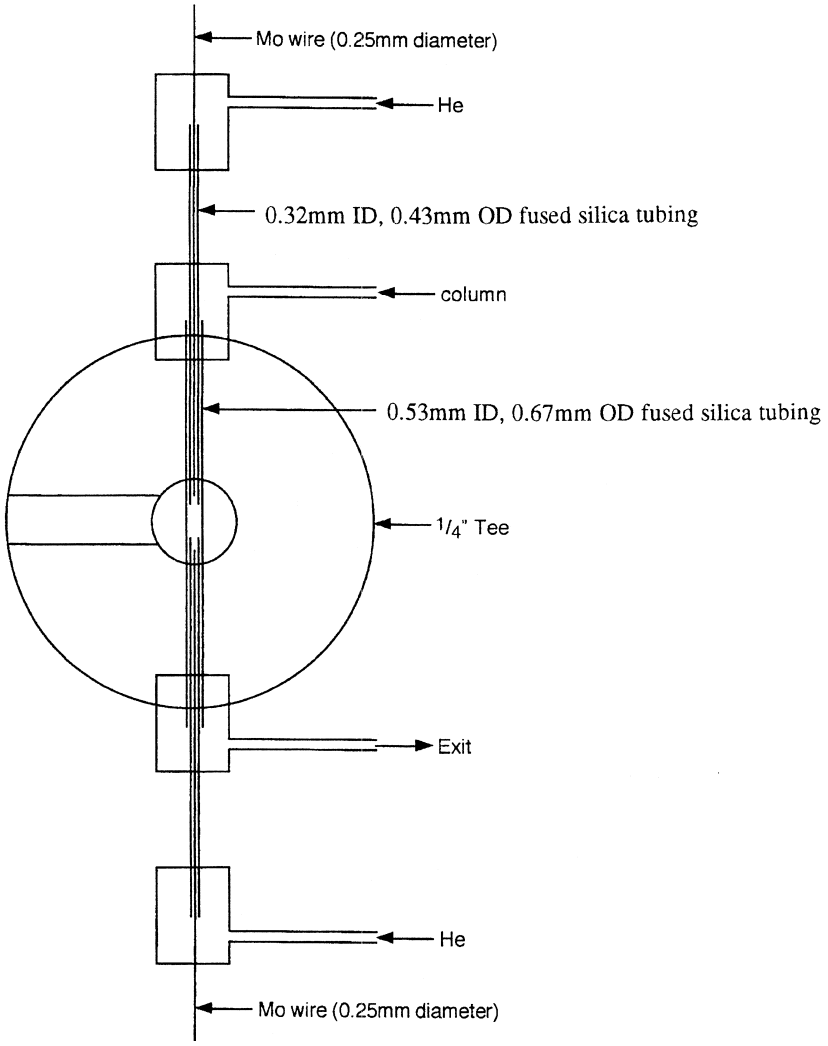

Fig. 4. Cross section of Cl-PDED.

portion of the spectrometer was the Acton monochromator which was made by Acton (Acton Research, Acton, MA, USA) specifically for spectral measurements in the range of 100–250 nm. It has a 1/8 m optical path as shown in Fig. 3. The grating contains 2400 groves/mm and is blazed at 150 nm. All optics are No. 1200 $AlMgF_2$ coated. As mentioned earlier, the PDED was attached to the entrance so that the discharge was at the position where the entrance slit is normally placed. The exit slit was variable and was set at 0.050 mm. An EMI 9781 B photomultiplier (EMI Gencom, NY, USA) was used to measure the spectral intensities. A high voltage of 650 V was applied to the PMT. The spectral range of the photomultiplier was 180–650 nm. The current from the photomultiplier was sent to a HNU Model PI-52 electrometer (HNU system, Newton, MA, USA) and the voltage (0–10 V) from the electrometer was sent to the computer.

For the wavelength scan of emission spectra from He, Kr, Cl and KrCl* a GCA/McPherson EU700 monochromator (GCA/McPherson Instruments, Acton, MA, USA) was used. The monochromator contains a 1200 lines/mm grating and is blazed at

250 nm with a dispersion of 2 nm/mm and maximum resolution of 0.1 nm at 250 nm. The same photomultiplier EMI 9781 B was used to measure the emission spectra from 180 to 650 nm.

2.3. Gas chromatograph

A Hewlett-Packard HP5880 gas chromatograph was used. All samples were liquids and were injected through the splitter. None of the detectors that came with the instrument were used. A J&W DB-5.625 capillary column 30 m×0.25 mm I.D., film thickness 0.5 μm was used for the analysis of volatile compounds. The end of the column was inserted into a piece of megabore fused-silica tubing (30 cm×0.53 mm I.D.) connecting the Cl-PDED. Kr-doped helium, at flow-rates between 0.5~8 ml/min, was mixed with the column effluent to provide the Kr-doped reaction gas and to overcome the small dead volume in the Tee through which the column effluent passes.

The signal (voltage) from the electrometer was converted to a digital output through a SMAD II (21 bits) A–D converter 02A (Marc S. Nathanson, Sharon, MA, USA)., and processed through The Chromatography Data Acquisition System for the Macintosh, Machrom V2.02A (Marc S. Nathanson). A Macintosh Performa 6214CD computer was used.

2.4. Pulse generator

The same pulse generator as described in the paper by Wentworth et al. [13] was used in this study. The high voltage required for the discharge was supplied by an automotive coil (E-30 Borg Warner). The coil was charged with 20 V from a Heathkit 2718 tri-power supply unit (Heath, Benton Harbor, MI, USA). The frequency of the discharge and the charging time of the coil were controlled by a 4001 ultravariable pulse generator (Global Specialties, New Haven, CT, USA).

3. Mechanism of chlorine selective detection

3.1. Mechanism of helium excitation in a pulsed discharge

An emission spectrum from He in the UV–visible region obtained by the Cl-PDED at atmospheric exit pressure is shown in Fig. 5. The presence of many nitrogen bands indicates that there is greater back diffusion of air at such a low detector flow-rate of 5 ml/min for this new version detector, compared to 30~50 ml/min for the conventional pulsed discharge emission detector [12,14–16]. This does not affect the Cl-PDED performance since the effect of nitrogen bands from back diffusion is almost offset by doping Kr into He in the discharge as shown in Fig. 6.

A comprehensive spectroscopic study of the emission spectra arising from the pulsed discharge has been carried out by Wentworth et al. [16]. From the

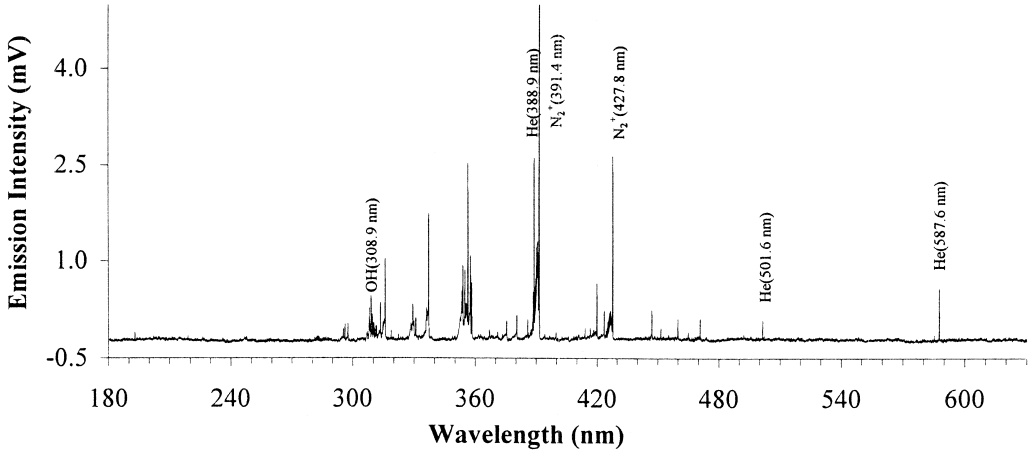

Fig. 5. UV–visible emission spectrum of helium at 1 atm (=101 325 Pa) pressure obtained by Cl-PDED. Pulse width: 30 μs, pulse spacing: 400 μs, discharge gas: helium, flow-rate: 5 ml/min, detector temperature: 30°C.

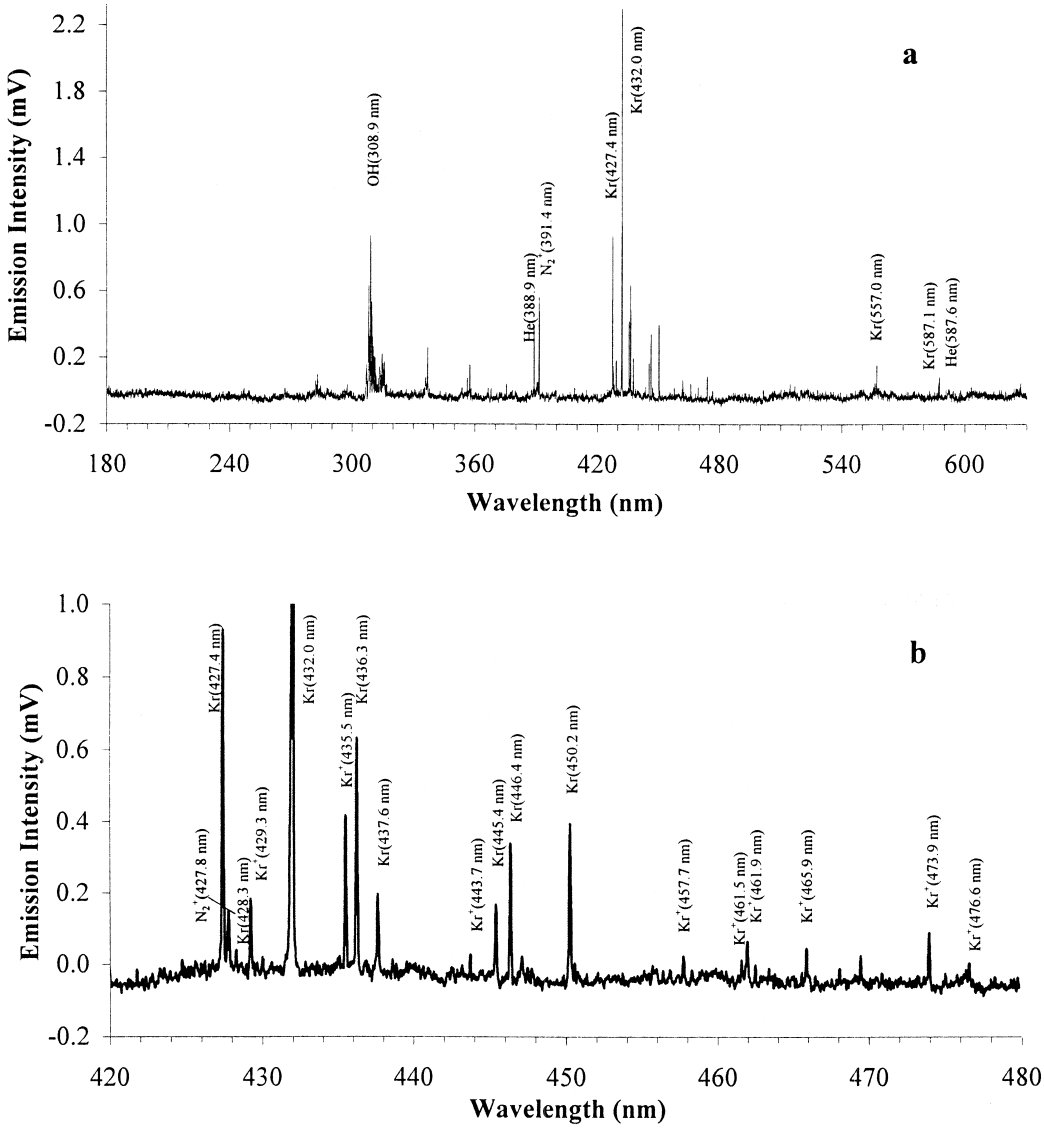

Fig. 6. (a) UV–visible emission spectrum of krypton-doped helium at 1 atm pressure obtained by Cl-PDED. Pulse width: 30 μs, pulse spacing: 400 μs, discharge gas: 0.4% krypton in helium, flow-rate: 5 ml/min, detector temperature: 30°C. (b) Emission spectrum of krypton-doped helium near 440 nm. Same conditions as in (a).

results of that study a mechanism for the production of excited and ionized species has been proposed. Summaries of the essential features of the mechanism that are pertinent to this work are as follows:

1. He* emission intensities correlate with a Boltzmann distribution of the He* states. The correlation gives an estimate of the discharge temperature of 3200 K.
2. The ionization in the discharge arises primarily by the following reaction of helium atoms in an excited triplet state: $2He(2^3S) \rightarrow He^+ + He + e^-$
3. The stability of the discharge is apparently due to the lack of ionization directly by the discharge.
4. He_2^* comes from two reaction paths:

(a) $He^* + 2He \rightarrow He_2^* + He$ (1)

$$(b)\ He^+ + 2He \rightarrow He_2^+ + He \quad (2)$$

$$He_2^+ + e^- \rightarrow He_2^* \quad (3)$$

The He_2^* generated in Eq. (1) fits a Boltzmann distribution since He* follows a Boltzmann distribution. He_2^* formed in Eq. (2) does not fit a Boltzmann distribution. The He_2^* formed by these processes can be differentiated by following the He_2^* emission as a function of time when a negative discharge potential is used.

Since the discharge is carried out at approximately one atmosphere pressure, this relatively high concentration of He probably converts most of the He* and He^+ to He_2^* and He_2^+, respectively. The concentration of He_2^+ will be enhanced by using a negative discharge potential that repels the electrons from the discharge region.

3.2. Mechanism of excitation in krypton-doped helium

If helium is doped at low concentrations of krypton (<1%) the physical characteristics of the discharge remain the same as in pure helium. This logically results since the initial excitation will occur with the major component, i.e., helium. The excited He species then transfer their energy to the lower energy states of Kr. The lowest excited states of Kr are at 11.1 and 11.6 eV, and these are readily observed from the vacuum ultraviolet emission spectra of Kr-doped helium [12]. Of course excited states of Kr above the lowest excited state could also be formed. These would range up to the ionization limit of 13.999 eV for Kr. Transitions from these upper excited states to the lower excited states would give off radiation in the visible region with $\lambda > 428$ nm. Indeed we have recorded the emission spectrum from Kr-doped helium and some of these transitions are shown in Fig. 6. The emission spectrum also contains some He transitions but they are of lower intensities than in pure He. The most intense He emission occurs at 388.9 nm. The line at 557.0 nm comes from Kr. The group of lines in the vicinity of 440 nm arises from krypton. The four intense lines 427.4, 432.0, 435.5 and 436.3 nm could be attributed to Kr or Kr^+ since both species have transitions at these wavelengths.

From this spectrum it is obvious that both excited Kr and Kr^+ are formed in the discharge. Either He_2^* or He_2^+ has sufficient energy to form these species in a Kr-doped helium mixture:

$$He_2^* + Kr \rightarrow Kr^+ + 2He + e^- \quad (4)$$

$$He_2^+ + Kr \rightarrow Kr^+ + 2He \quad (5)$$

Ionization of Kr requires the ionization potential of 13.999 eV. The He_2^* states are ~18 eV and higher [17]. The energy available from He_2^+ is the ionization potential of He (24.5 eV) minus the bond energy of He_2^+ (2 eV) which gives 22.5 eV, far in excess of the required 13.999 eV. The above reactions could occur starting with the monatomic species He* and He^+ and the energetics would be even more favorable. However, we think the diatomic species are the most predominant at one atmosphere helium. Even though we give two processes for the formation of Kr^+ in Eqs. (4) and (5) we think Eq. (5) would make the largest contribution since ion–molecule reactions are inherently faster than reactions of neutral species. The excited monatomic Kr can also be produced but that would probably be through a reaction of neutrals:

$$He_2^* + Kr \rightarrow Kr^* + 2He \quad (6)$$

Since we observed emission from Kr* in the UV–visible region in addition to the resonance radiation in the vacuum UV, the upper electronic states must be occupied at energies just under the ionization potential (*IP*). Hence the energy required to excite Kr would be less than the *IP* of 13.999 eV. As mentioned previously, He_2^* states are at 18 eV or higher so there is more than enough energy to allow the reaction in Eq. (6) to occur.

*3.3. Mechanism of formation of KrCl**

When a chlorocompound is introduced to the pulsed discharge in Kr-doped helium we observe the well known emission from KrCl* at 221–222 nm. The emission spectrum for the molecular transition of KrCl* is shown in Fig. 7. The emission spectrum of chlorine in pure helium is shown in Fig. 8 for comparison. The spectrum of KrCl* obtained through the pulsed discharge is similar to those

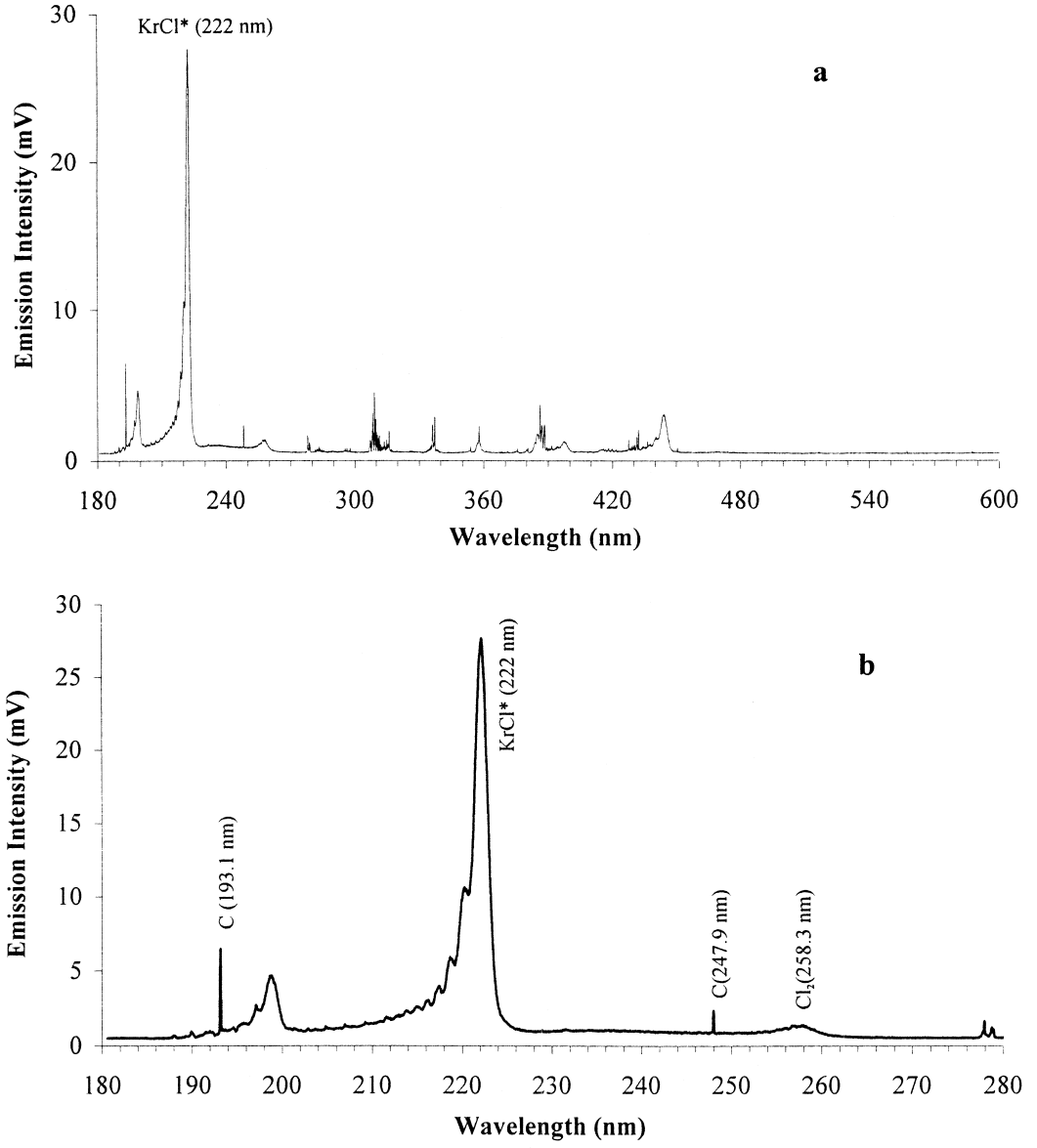

Fig. 7. (a) Emission spectrum of KrCl* at 1 atm pressure obtained by Cl-PDED. Pulse width: 30 μs, pulse spacing: 400 μs, reaction gas: 0.8 ppm CH_2Cl_2 in krypton-doped helium (0.4% Kr), flow-rate: 5 ml/min, detector temperature: 30°C. (b) Enlarged emission spectrum of KrCl*. Same conditions as in (a).

obtained in other exciting sources [9–11]. The KrCl* emission band with a half width of 1.7 nm shows only a small amount of rotational fine structure on the short wavelength side. Note that the KrCl* emission is far removed from the atomic carbon emission at 193.1 nm. There are, however, a few C_2^* emissions in the vicinity of 221–222 nm that can possibly interfere with the measurement of the KrCl* emission.

From an energetics standpoint both Kr* and Kr^+

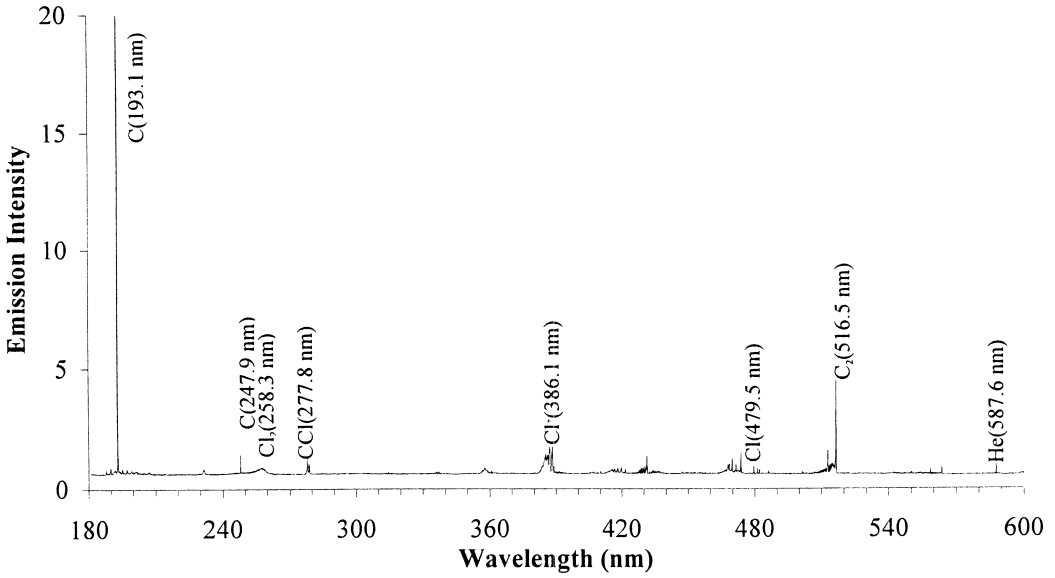

Fig. 8. Emission spectrum of chlorine in helium at 1 atm pressure obtained by Cl-PDED. Pulse width: 30 μs, pulse spacing: 400 μs, reaction gas: 4 ppm CH_2Cl_2 in helium, flow-rate: 5 ml/min, detector temperature: 30°C.

could abstract the Cl from a organochlorine compound to form the excited state of KrCl*. For the reaction with Kr*

$$Kr^* + RCl \rightarrow KrCl^* + R^{\cdot} \quad (7)$$

the change in energy for the process is

$$\Delta E = -E^*_{Kr} + D_{R-Cl} - D_{Kr-Cl^*} \quad (8)$$

$$\Delta E = -10.1\ eV + 3.5\ eV - 3.4\ eV = -10.0\ eV \quad (9)$$

where we have estimated the R–Cl bond dissociation energy as 3.5 eV (~80 kcal/mol; 1 cal = 4.184 J) and the Kr–Cl* bond dissociation energy as $3/2\ D_{Br-Cl} =$ 3.4 eV. The Kr–Cl* should have a bond order of 3/2 since an antibonding electron has been promoted to a bonding molecular orbital in the excited state. Obviously the process is highly exothermic and would be so regardless of the estimates in the bond dissociation energies.

For the reaction with Kr^+

$$Kr^+ + RCl \rightarrow KrCl^* + R^+ \quad (10)$$

the change in energy can be estimated by

$$\Delta E = -IP_{Kr} + D_{R-Cl} - D^*_{Kr-Cl} + IP_R \quad (11)$$

$$\Delta E = -13.999\ eV + 3.5\ eV - 3.4\ eV + (7–9)\ eV$$
$$= -6.9\ \text{to}\ -4.9\ eV \quad (12)$$

where we have assumed a range for the *IP* of R to be from 7 to 9 eV. The *IP* from the propyl radical is 8.1 eV and isopropyl 7.5 eV, whereas the *IP* for the phenyl radical is 9.2 eV. Again we see that the process is highly exothermic, regardless of the estimates in the bond dissociation energies and the *IP* of the radicals. Both the reactions with neutral He* and the ion He^+ would be favorable from a thermodynamic standpoint. However, we know that the ion–molecule reaction should occur at a faster rate due to the ion-induced dipole interactions. For this reason we think the principal source of KrCl* is through the reaction given by Eq. (10).

4. Effects of operating parameters on chlorine-selective pulsed discharge emission detector

The Cl-PDED has several operating parameters that affect the sensitivity and the selectivity of the detector. Two of them are involved with the spectrometer: wavelength selection and exit slit width. Another three parameters are associated with the

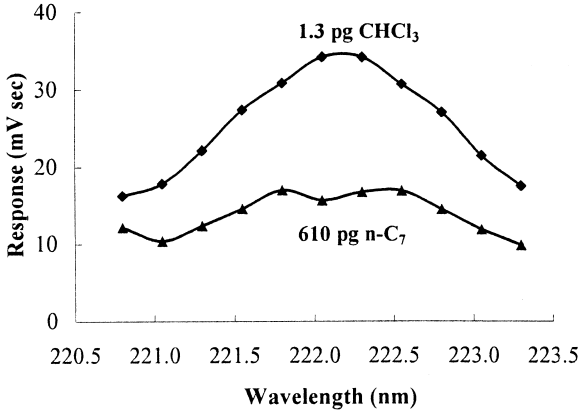

Fig. 9. Effect of wavelength on response. Discharge gas: 0.2% krypton in helium, flow-rate: 3.8 ml/min.

pulsed discharge: the pulse width, the pulse spacing and polarity of the pulsed discharge. Other operating parameters include Kr concentration, detector temperature and detector flow-rate. For a new Cl-PDED it must be purged with helium for tens of hours to reach a constant response. All of these operating parameters will be discussed according to the detector sensitivity as well as the selectivity to find the optimum operating conditions.

4.1. Wavelength

The choice of the detection wavelength affects both the sensitivity and the selectivity. In Fig. 9 we show the Cl response as well as the response of carbon interference from 220.5 to 223.5 nm. The maximum Cl response occurs at the wavelength of 222.1 nm. The Acton monochromator used for this study was calibrated by the carbon line of 193.1 nm and by comparison with the GCA/McPherson EU 700 monochromator. This maximum wavelength of KrCl* emission is identical with that reported by Jones et al. [11]. Since there are possible C_2 emissions at 221.66 and 221.82 nm [18], and the carbon continuum to interfere with the Cl detection in this wavelength region, it is critical to consider not only the sensitivity of Cl detection but also the selectivity to carbon with respect to the selection of the wavelength. Fortunately, at the wavelength of 222.1 nm both the elemental response of chlorine and the selectivity to carbon are highest, as shown in Fig. 10. It is also shown in Figs. 9 and 10 that the correct selection of the wavelength is important since the response varies rapidly with the wavelength. In this study a wavelength of 222.1 nm (calibrated wavelength for the Acton Monochromator used in this work) was used except in one case where 222.6 nm was used instead to study the effect of detector temperature on response.

4.2. Monochromator slit width

Since the entrance slit was eliminated due to the narrow discharge of the Cl-PDED detector, only the exit slit of the monochromator was considered. The exit slit controls the light intensity collected by the photomultiplier. Although a large exit slit width

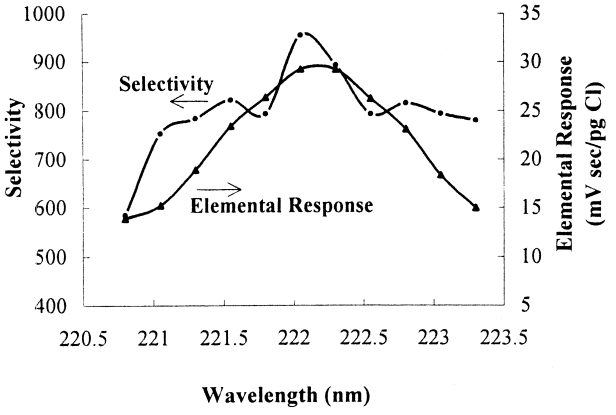

Fig. 10. Effect of wavelength on selectivity and elemental response.

increases the detection intensity, it raises the background and noise levels and lowers the spectral resolution. It has both positive and negative effects on the Cl-PDED performance. In Fig. 11a we show the elemental response to chlorine and the selectivity to carbon at various slit widths. Since the emission intensities of KrCl*, the carbon interference from C_2, and the carbon continuum increase proportionally with the slit opening, the selectivity remains nearly unchanged. The higher response at the larger slit due to the greater light intensity does not necessarily mean an improvement in detector performance since, on the other hand, the detector performance deteriorates due to the higher background and noise levels. Fig. 11b shows a graph of the minimum detectability to chlorine versus the exit slit, which reflects both effects of the signal intensity and the noise level on the detector performance. The minimum detectability varies slightly from a slit width of 65 to 200 μm. To reduce the possibility of spectral interference from other elements except Cl, such as C, N and O, an exit slit width of 50 μm was used in this study.

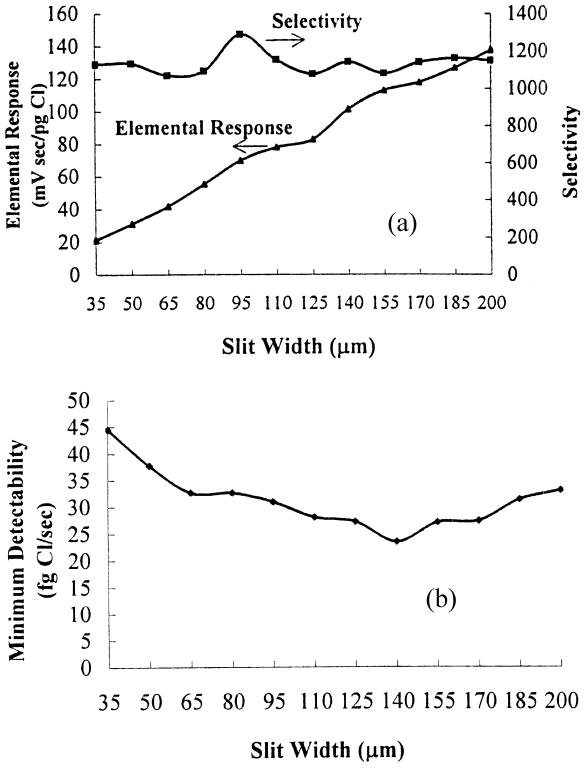

Fig. 11. (a) Effect of slit width on selectivity and sensitivity. Discharge gas: 0.2% krypton in helium, flow-rate: 3.8 ml/min. (b) Effect of slit width on minimum detectability.

4.3. Pulse width and spacing

For the Cl-PDED the spacing between the discharge electrodes is 1.6 mm. The discharge reaction region consists of a piece of megabore fused-silica capillary tubing with 0.53 mm I.D. The volume of the reaction region through which the Kr-doped helium and compounds pass is very small, about 0.35 μl. This small volume helps to spatially confine the discharge, enhance current density and brightness and to allow the use of a lower helium flow-rate. As a result of the high current density for the Cl-PDED, the pulsed discharge needs less power applied to it compared to other pulsed discharge detectors (PDED [12,14,15], helium pulsed discharge photoionisation detector [13] and pulsed discharge electron-capture detector [19,20]).

The current and voltage of the discharge are controlled by two factors: (1) the power supplied to the discharge via the primary coil and (2) the frequency of the pulsed discharge. The power supplied to the discharge depends upon the time that a 20-V power supply is applied to the coil. This is controlled by the pulse width of a square wave pulse generator. The frequency of the discharge is controlled by the frequency of the pulse supplied by the square wave pulse generator. Generally, a larger pulse width raises baseline and noise levels, the sensitivity increases as the pulse spacing is lowered. However, the noise level also must be considered. The baseline level and the noise level were measured at different combinations of the pulse width and the pulse spacing. A pulsed discharge with a 15-μs width and a 400-μs spacing has both lower levels of the baseline and the noise, and at the same time has a moderate power supplied to the discharge. Thus, it was used in the study except where indicated.

4.4. Polarity of pulsed discharge

The polarity of the pulsed discharge affects the baseline and the noise dramatically, as shown in Fig. 12. A negative pulsed discharge resulted in a noisy background and a chromatogram with distorted

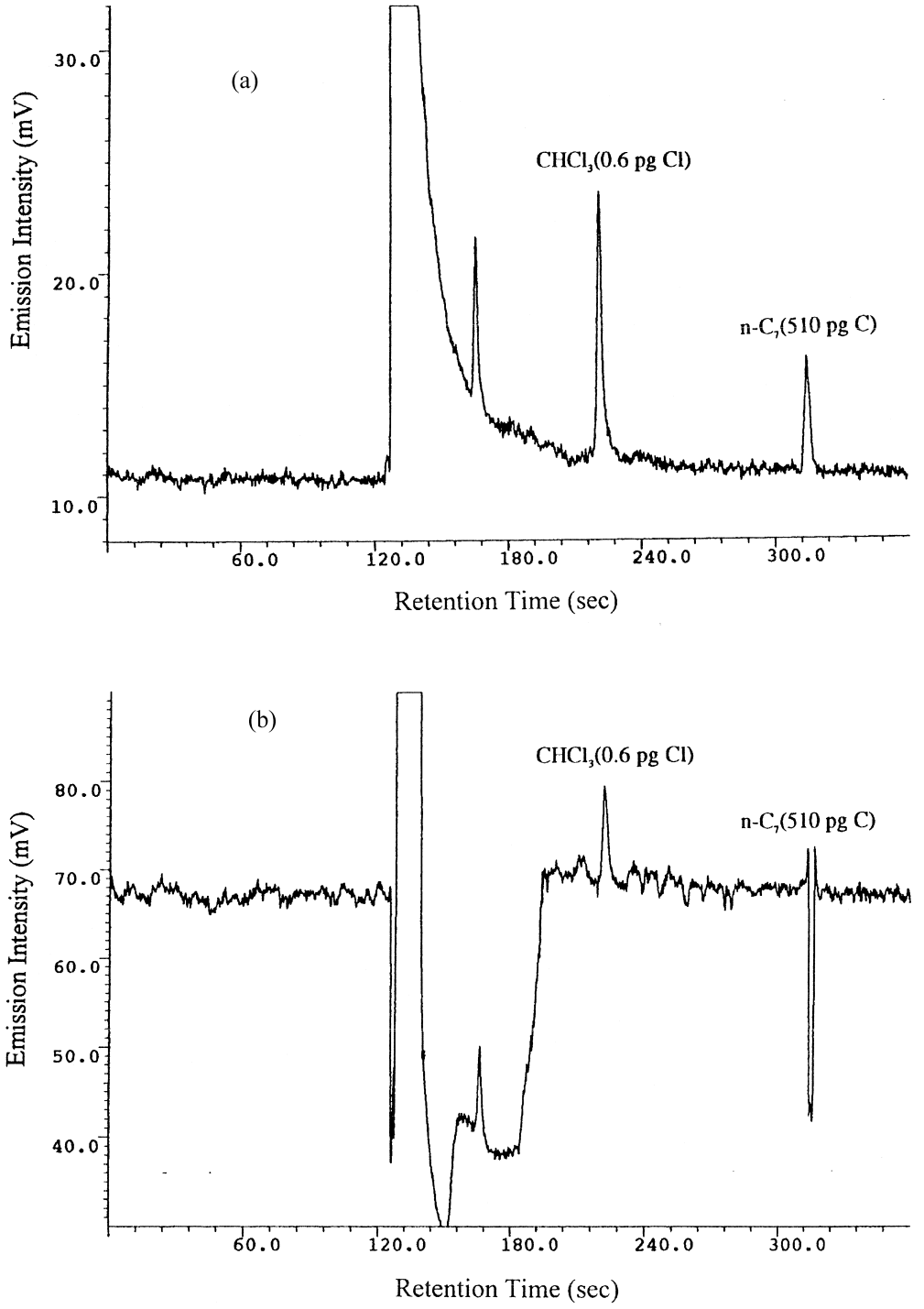

Fig. 12. (a) Chromatogram using the Cl-PDED with a positive pulsed discharge. Column: DB-5.625, 30 m×0.25 mm I.D., d_f: 0.5 μm, carrier gas: He, flow-rate: 25 cm/s, column temperature: 55°C, injector temperature: 150°C, pulse width: 15 μs, pulse spacing: 400 μs, wavelength: 222.1 nm, discharge gas: 0.1% krypton in helium, flow-rate: 6 ml/min, detector temperature: 130°C. (b) Chromatogram using the Cl-PDED with a negative pulsed discharge. Same conditions as in (a).

peaks (Fig. 12b). It is obvious that a positive pulsed discharge is preferable over a negative pulse discharge.

4.5. Purging time for the new detector

For a newly built Cl-PDED, water and air are adsorbed on the inside surface of the detector and it takes a considerable period of time to purge the detector with helium prior to its use. Fig. 13 shows a graph of the elemental response to chlorine versus the purging time. The response was considerably lower at the beginning, and it took at least 2 days before the response increased to a constant value. Since the total detector flow-rate is small, ca. 5 ml/min, we suggest that the detector be purged with helium continuously, even when not in use.

4.6. Krypton concentration

The response of the Cl-PDED was measured as a function of Kr concentration for eight compounds. The Kr concentration was varied from 0.1 to 1.0% in intervals of 0.1%. The average elemental response from five runs for each compound as a function of Kr concentration is shown in Fig. 14. In general there is little change in response with concentration of Kr for all eight compounds. Above 0.3–0.4% there is a gradual decrease in response, but the overall change to 1% Kr is only about 7%. From these results a concentration of ~0.2% Kr is satisfactory and slight variations in the Kr concentration should have little effect on the response. For these studies the detector temperature was 130°C and the flow-rate through the detector was 4.3 ml/min. Approximately 5 pg of each compound was injected, which, as we will see later, is well within the linear concentration range. A DB-5.625 column (30 m × 0.25 mm I.D. and 0.5 μm thickness from J&W Scientific) was used for the separation. The temperature program was isothermal at 40°C for 2 min, 20°C/min to 140°C and held at 140°C for 3 min.

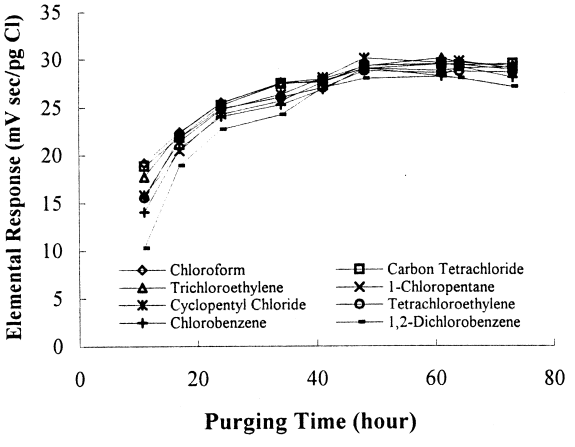

Fig. 13. Elemental response versus purging time.

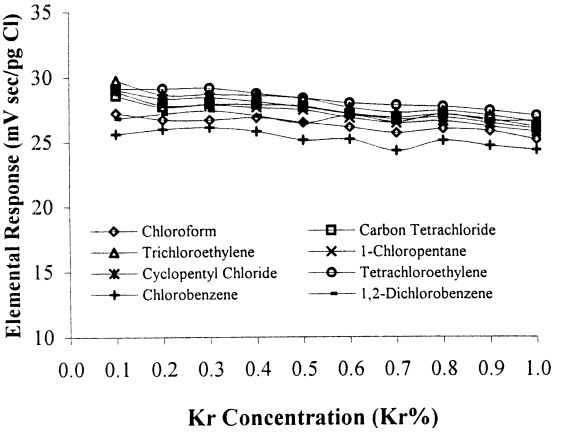

Fig. 14. Elemental response versus Kr concentration. Discharge gas flow-rate: 4.3 ml/min, 5 pg Cl of each compound.

4.7. Detector temperature

Elemental response has been studied as a function of temperature in the range 40–160°C. For these studies the wavelength was 222.6 nm, the Kr concentration was 0.4%, the flow-rate was 4.8 ml/min and ~20 pg of each compound was injected. Other conditions were the same as in Fig. 18. There is no significant trend for any of the eight compounds over the temperature range investigated. Since the response should be directly related to the rate for the $Kr^{+} + RCl$ reaction, the activation energy for this reaction must be approximately zero. From an analytical standpoint the detector temperature is insignificant except that it must be sufficiently high to prevent condensation of the compounds being eluted. In order to examine the slight variations with temperature, the average elemental response is graphed

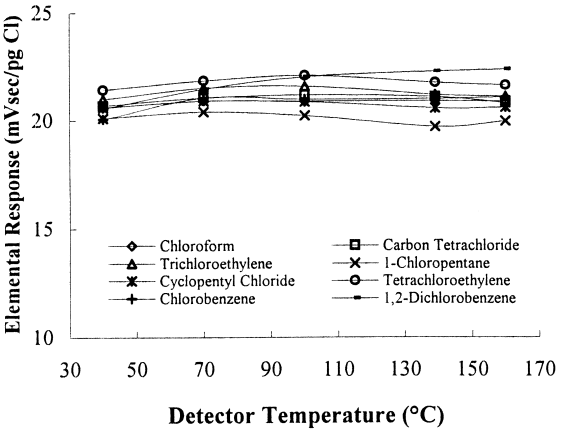

Fig. 15. Elemental response versus detector temperature. Discharge gas: 0.4% krypton in helium, 4.8 ml/min, 20 pg Cl of each compound.

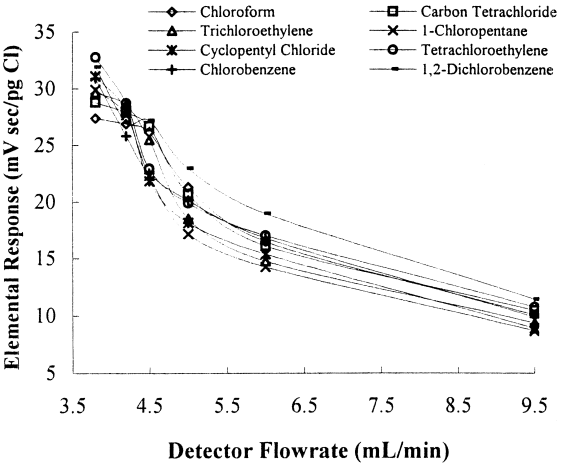

Fig. 16. Elemental response versus detector flow-rate. Discharge gas: 0.35% krypton in helium, 5 pg Cl of each compound.

as a function of temperature in Fig. 15. Again the average response is the average of five runs for each of the eight compounds. Raising the temperature from 40 to 70°C increases the average response of the eight compounds by 2.5% but increasing the temperature in steps to 160°C shows no significant change in response. There is, however, a slight increase in the variation of response from one compound to another as the temperature is increased, but again the increase is not significant. Based on these data we can conclude that the response of the Cl-PDED detector is essentially independent of temperature.

4.8. Detector flow-rate

The dependence of the elemental response on flow-rate is shown in Fig. 16. For these studies the detector temperature was 130°C, Kr concentration was 0.35% and approximately 5 pg of each compound was injected. Other conditions were the same as in Fig. 18. Again the average of five response values is given for each compound at flow-rates (F) ranging from 3.8 to 9.5 ml/min. Since the response of the Cl-PDED detector is certainly concentration dependent, the response decreases with increasing flow-rate. One would expect the response to be proportional to the reciprocal of the flow-rate, as shown in Fig. 17. The expected linear relationship is better obeyed at high flow-rates or low reciprocal flow-rates. The response/pg Cl seems to become greater than expected by the $1/F$ relationship as shown by the upward curvature in Fig. 17 at large $1/F$ values. If the objective is to obtain the maximum sensitivity, a low flow-rate would be desired. Since the response is quite sensitive to flow-rate at 4–4.5 ml/min, the flow-rate should be well controlled in order to have good reproducibility.

We summarize typical operating conditions as follows:

- Wavelength: 222.1 nm.
- Monochromator slit width: 50 μm.

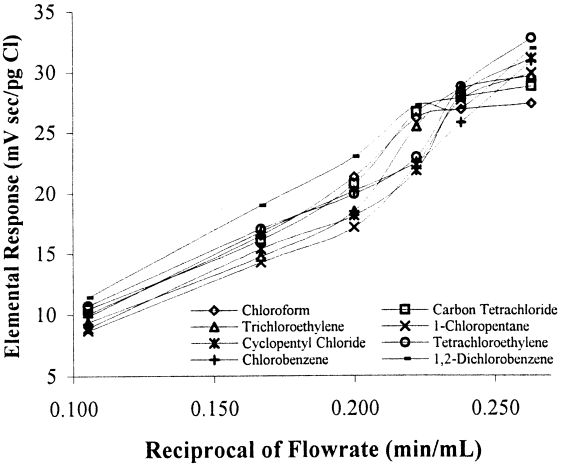

Fig. 17. Elemental response versus reciprocal of flow-rate.

- Pulse width and spacing: 15 μs/400 μs.
- Polarity of pulsed discharge: positive.
- Krypton concentration: 0.1~0.5%.
- Detector temperature: insensitive.
- Detector flow-rate: 4~5 ml/min.

5. Performance of Cl-selective pulsed discharge emission detector

As discussed earlier, the Cl-PDED is a selective detector, which responds only to the presence of chlorine atoms in a compound. The response of the Cl-PDED is especially sensitive to the detector flow-rate, generally decreasing with increasing detector flow-rate. This clearly indicates the Cl-PDED, like other atomic emission detectors, is a concentration dependent detector.

5.1. Sensitivity and minimum detectability

As mentioned earlier, the Cl-PDED is a concentration detector. In the literature, however, the atomic emission detector (AED) was treated as a mass flow detector although it is a concentration detector. For comparison with the AED and other GC detectors, the results in Table 1 are given in both concentration and mass units.

The Cl-PDED sensitivity is the highest of the element-selective detectors (Hall, AED, halogen selective detector (XSD), nitrogen–phosphate and flame photomeric detectors). The minimum detectability to chlorine is 50 fg/s. The Cl-PDED sensitivity is greatly enhanced due to three unique features: (1) the reaction of krypton with chlorine is an ion–molecule reaction which is 100–1000 times greater than a reaction of neutrals; (2) the discharge reaction region consists of a piece of capillary tubing with a volume of 0.35 μl which spatially confines the discharge to enhance the discharge density and brightness; (3) the discharge is sufficiently narrow that it replaces the entrance slit to the monochromator, which greatly enhances the light gathering power.

In Fig. 18 we show chromatograms of the eight component mixture used in Tables 1 and 2 and Figs. 13 – 17. Fig. 18a results from the injection of approximately 0.1 pg of Cl for each of eight components. In Fig. 18b, we show a similar chromatogram except that the level of injection was approximately 50 pg of Cl for each compound. The signal-to-noise ratio for the compounds shown in Fig. 18a is about 5:1, and the peak half widths are around 1.7 s, so we estimate the detection limit as 50 fg Cl/s at the signal-to-noise level of $S/N=3$.

5.2. Linear range and dynamic range

In Fig. 19 we show the linear range and the dynamic range of chloroform for the Cl-PDED. Fig. 20 shows the linear range in detail at low concentrations of chloroform. As shown in the figures, the Cl-PDED linear range is over 2000 and the dynamic range is extended to 15 000.

Scott and Fowliss [21] proposed a method for linearity measurement, which can be expressed by the following simple relationship: $y = ax^b$ where y is response (mV s), x is mass injected (pg), a is a constant and b is the response index.

The response index b provides an accurate measure of linearity. For a truly linear detector, b will be unity. If the response index b falls between 0.98 and 1.02 the detector response can be assumed to have a satisfactory linearity.

The response as a function of concentration for all eight compounds within the linear range is combined in a single graph of log R versus log pg Cl in Fig. 21. By combining the data into a single graph one can evaluate the variation in response from different compounds along with the variation in the data. In

Table 1
Sensitivity and minimum detectability of Cl-PDED

Concentration		Mass	
Sensitivity [mV/(g Cl/ml)]	Minimum detectability [g Cl/ml]	Sensitivity [mV/(g Cl/s)]	Minimum detectability [g Cl/s]
$2.4\cdot10^{12}$	$5.0\cdot10^{-13}$	$2.5\cdot10^{13}$	$5.0\cdot10^{-14}$

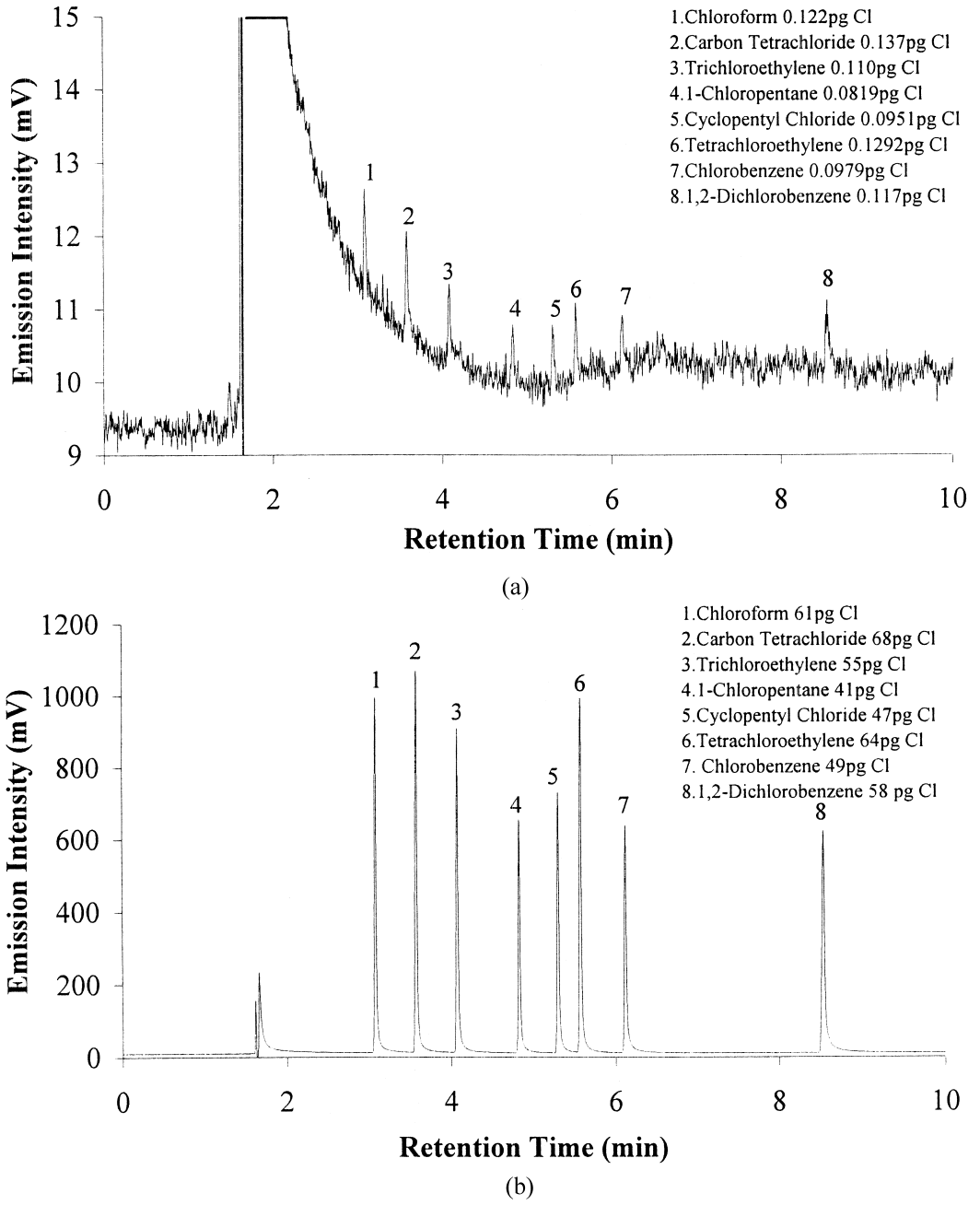

Fig. 18. Chromatograms of eight chlorinated compound mixture using the Cl-PDED. (a) Low concentration, (b) high concentration. Column: DB-5.625, 30 m×0.25 mm I.D., d_f: 0.5 μm, carrier gas: He, flow-rate: 30 cm/s, oven temperature program: 40°C (2 min), 20°C/min to 140°C (3 min), pulse width: 15 μs, pulse spacing: 400 μs, wavelength: 222.1 nm, detector gas: 0.2% krypton in helium, detector flow-rate: 4.2 ml/min, detector temperature: 150°C, injector temperature: 150°C, injector split ratio: 82:1, 0.2 μl sample in methanol.

Table 2
Elemental response versus mass of chlorine for eight compounds

Chloroform											
pg Cl[a]	0.122	0.354	0.708	1.409	6.776	12.94	29.59	99.60	142.29		
R/pg Cl[b]	24.99	26.38	25.99	25.74	25.35	25.83	26.39	25.96	24.79		
SD (*N*=5)	0.73	0.63	0.20	0.08	0.17	0.27	0.27	0.35	0.21		
RSD (%) (*N*=5)	2.91	2.38	0.78	0.32	0.67	1.05	1.01	1.34	0.83		
Carbon tetrachloride											
pg Cl	0.137	0.397	0.794	1.581	7.603	14.51	33.20	111.76	159.65		
R/pg Cl	25.67	26.57	26.60	27.73	27.13	27.41	26.34	26.27	23.98		
SD (*N*=5)	0.72	0.14	0.29	0.33	0.11	0.07	0.40	0.25	0.23		
RSD (%) (*N*=5)	2.81	0.53	1.08	1.20	0.42	0.25	1.52	0.94	0.98		
Trichloroethylene											
pg Cl	0.110	0.319	0.638	1.270	6.106	11.66	26.66	89.76	128.23		
R/pg Cl	24.04	26.23	25.92	26.54	25.96	26.32	25.50	25.96	24.68		
SD (*N*=5)	1.37	0.44	0.18	0.34	0.13	0.30	0.22	0.24	0.30		
RSD (%) (*N*=5)	5.71	1.69	0.68	1.27	0.49	1.13	0.87	0.93	1.22		
1-Chloropentane											
pg Cl	0.082	0.158	0.315	1.514	2.890	6.609	22.25	31.79	60.68	91.02	
R/pg Cl	25.34	27.30	26.66	25.83	25.47	24.87	26.77	25.59	24.48	21.33	
SD (*N*=5)	2.37	0.70	0.50	0.36	0.30	0.29	0.17	0.30	0.60	0.15	
RSD (%) (*N*=5)	9.36	2.58	1.88	1.39	1.19	1.16	0.65	1.18	2.43	0.69	
Cyclopentyl chloride											
pg Cl	0.095	0.184	0.366	1.758	3.357	7.677	25.85	36.92	70.49	105.74	
R/pg Cl	25.80	25.97	26.27	26.80	26.58	26.24	28.01	26.99	25.75	22.68	
SD (*N*=5)	1.32	0.97	0.66	0.29	0.38	0.17	0.24	0.25	0.49	0.14	
RSD (%) (*N*=5)	5.10	3.74	2.51	1.07	1.43	0.65	0.84	0.91	1.88	0.61	
Tetrachloroethylene											
pg Cl	0.129	0.374	0.748	1.490	7.164	13.68	31.28	105.31	150.44		
R/pg Cl	25.37	26.16	26.86	28.01	27.54	26.98	26.42	26.88	24.91		
SD (*N*=5)	0.85	0.20	0.76	0.18	0.09	0.07	0.30	0.18	0.22		
RSD (%) (*N*=5)	3.35	0.77	2.83	0.63	0.32	0.24	1.15	0.68	0.88		
Chlorobenzene											
pg Cl	0.098	0.189	0.376	1.810	3.455	7.901	26.60	38.00	72.55	108.82	
R/pg Cl	24.16	25.38	25.64	26.08	25.50	25.95	27.02	26.27	25.94	23.22	
SD (*N*=5)	1.19	0.66	0.60	0.17	0.37	0.13	0.30	0.30	0.19	0.21	
RSD (%) (*N*=5)	4.94	2.58	2.35	0.67	1.45	0.49	1.11	1.12	0.74	0.89	
1,2-Dichlorobenzene											
pg Cl	0.117	0.170	0.339	0.676	3.249	6.203	14.19	47.76	68.23	130.25	195.38
R/pg Cl	25.06	26.93	26.62	26.08	25.87	25.80	27.49	27.46	27.55	27.02	24.23
SD (*N*=5)	0.68	0.67	0.51	0.72	0.05	0.32	0.16	0.29	0.35	0.24	0.34
RSD (%) (*N*=5)	2.72	2.50	1.93	2.77	0.20	1.23	0.59	1.06	1.25	0.89	1.39
Overall average elemental response				25.97	± 1.17						

[a] Mass of chlorine injected.
[b] Average elemental response (mV sec/pg Cl) calculated from five measurements.

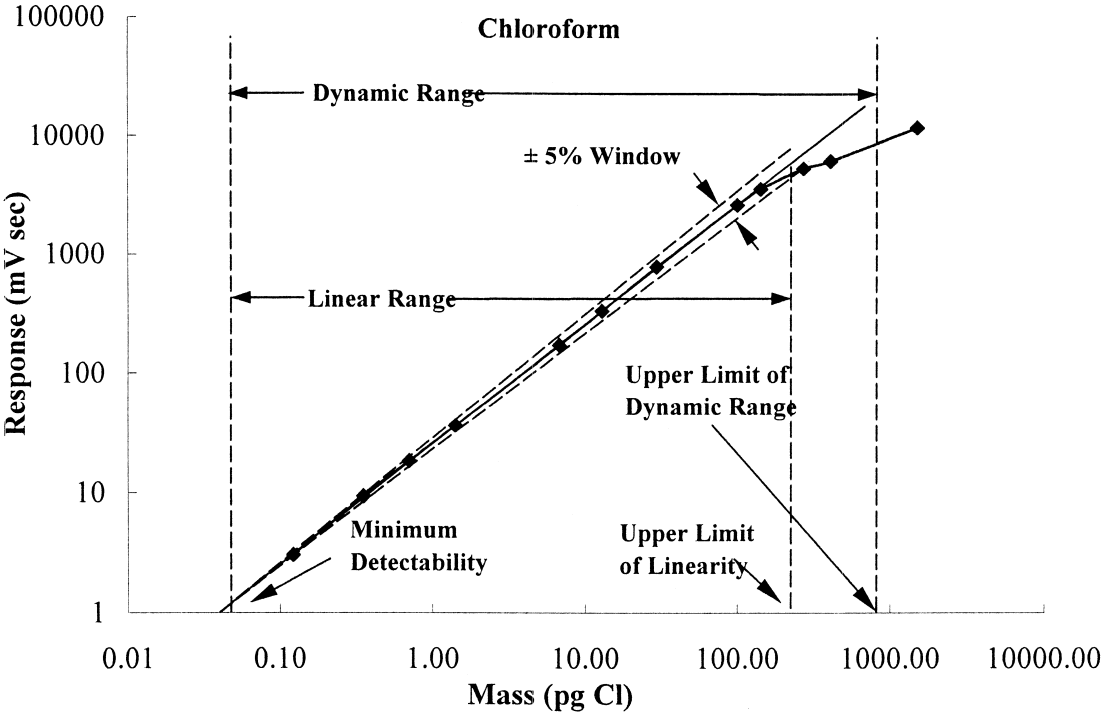

Fig. 19. Linear range and dynamic range of Cl-PDED. Same conditions as in Fig. 18.

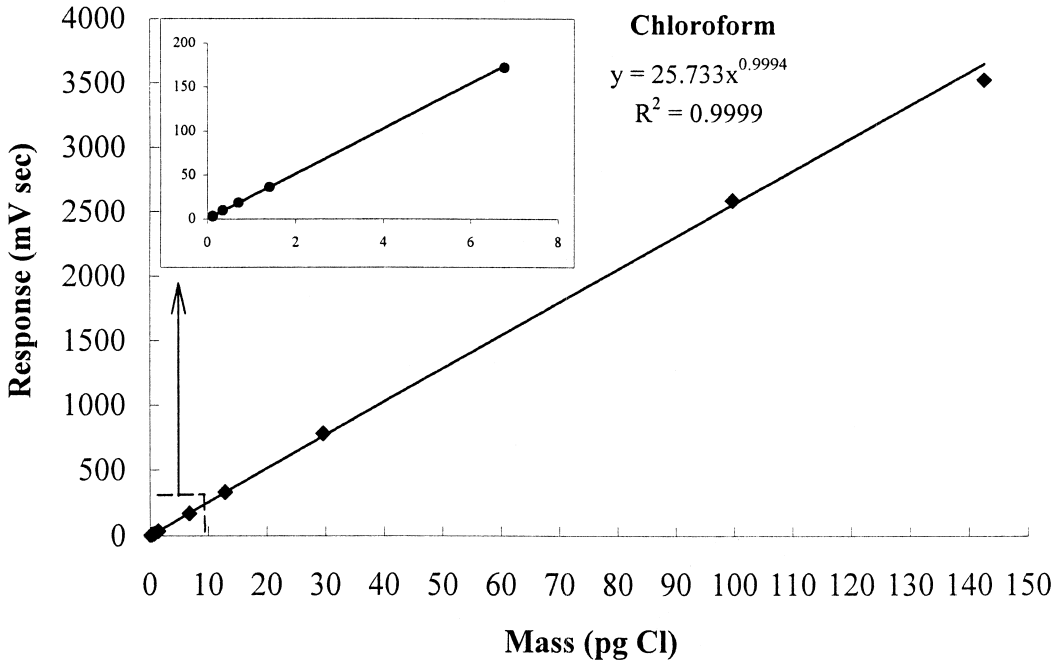

Fig. 20. Linearity at low concentrations. Same conditions as in Fig. 18.

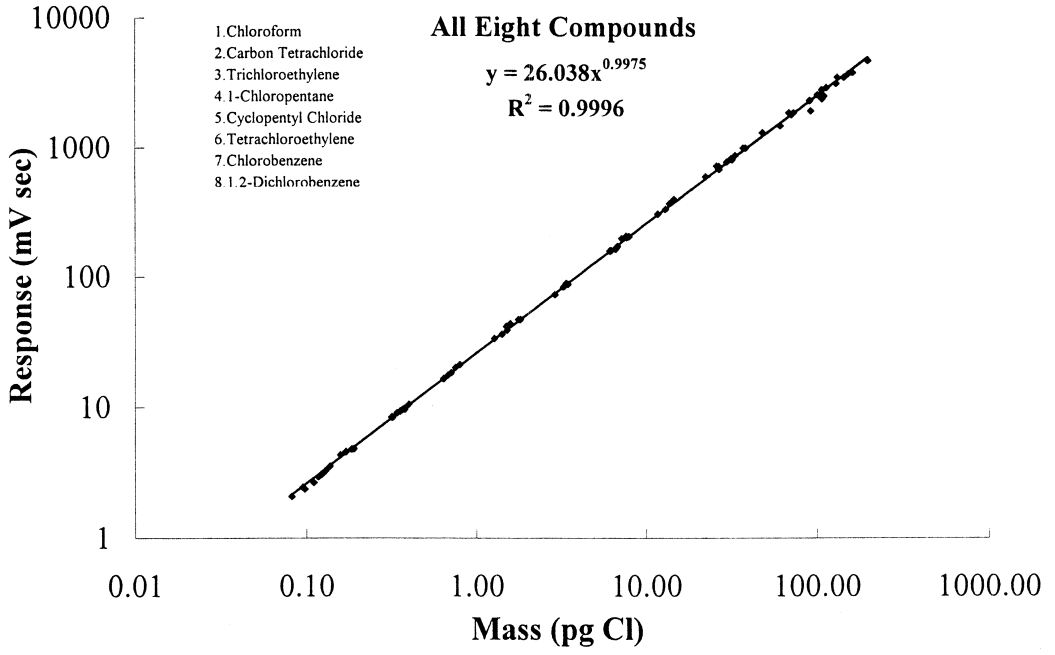

Fig. 21. Log response versus log pg Cl for all eight compounds. Same conditions as in Fig. 18.

Fig. 21 the average of five responses is shown at each concentration. The values of ''*a*'' show the consistency of the response/pg Cl. The values range from 25.419 to 26.646 for the individual eight compounds. The average of these ''*a*'' values is 26.038 with a percentage standard deviation of 1.7%. A reasonably good linear relationship with a response index of 0.9975 exists over three orders of magnitude from less than 0.1 pg Cl to ~150 pg Cl. Fig. 22 shows the dynamic range in a single graph for all eight compounds. Note that over four orders of magnitude are observed for the dynamic range in the combined graph of all eight compounds. This is consistent with the previously observed dynamic range of a single compound – chloroform.

Above 150 pg Cl the response curve bends over with a lower slope. The cause for the curvature above 150 pg Cl is most likely due to a decrease in the concentration of Kr^+ available for the reaction with RCl. In conclusion, the Cl-PDED response is linear over three orders of magnitude, and the dynamic range can be extended to four orders of magnitude.

5.3. Elemental response

The data in Table 2 are the elemental responses for all eight compounds within the linear range. Fig. 23 shows a graph of the elemental response versus mass of chlorine. The overall average elemental response is 25.97 mV s/pg Cl with a variation of ~4.5%. One should note the wide variety of compounds from saturated compounds with a large range of Cl substituents to unsaturated and aromatic Cl-containing compounds. This constant response/pg Cl suggests the rate constants involved in the excitation process are approximately constant, which is amazing considering the large variation in molecular structure and the C–Cl bond strength in the various compounds.

The data in Table 2 can also be used to evaluate the precision of the response/pg Cl. The standard deviation for the five successive measurements for each compound ranges from ~0.05 to 2.37 mV s with an average of ~0.40 mV s. For an average response/pg Cl of ~25.97 mV s/pg Cl, this is an average precision of ~1.5%. This, of course, is the precision

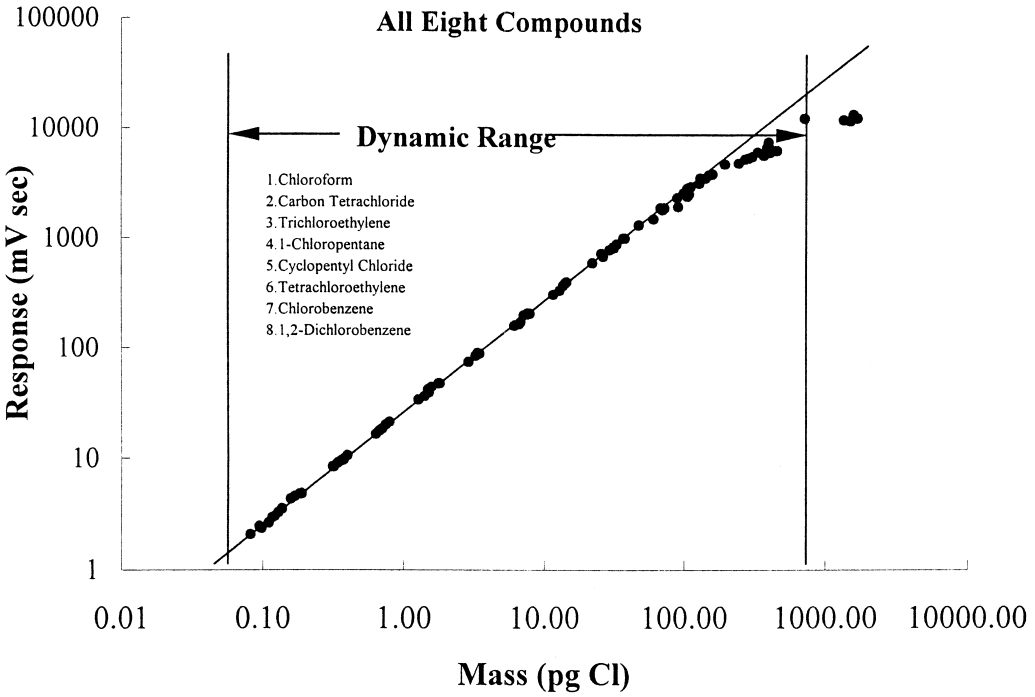

Fig. 22. Dynamic range for all eight compounds. Same conditions as in Fig. 18.

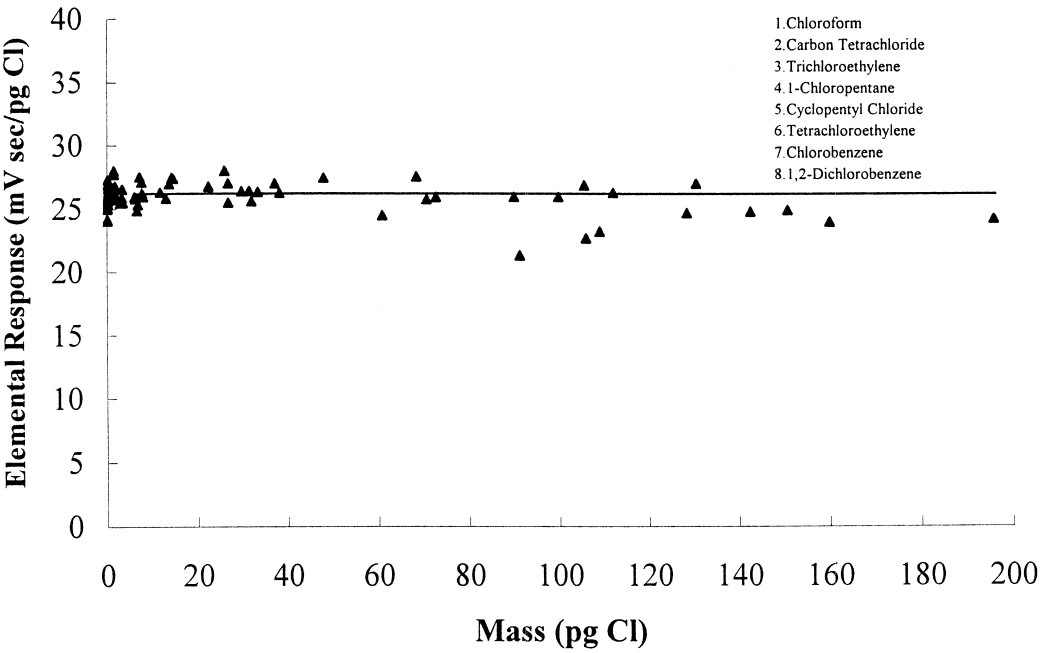

Fig. 23. Elemental response versus mass of chlorine. Same conditions as in Fig. 18.

over a relatively short term, and a subsequent study should be carried out in order to evaluate the precision over a long period of months to a year. The precision of the individual responses/pg Cl of 1.5% is lower than the 4.5% variation between compounds. Apparently the variation between compounds is real but is not much greater than the precision of the measurement.

5.4. Selectivity

The selectivity is used to measure the interference from the matrix. It is defined as the ratio of the response of chlorine to the response of the interfering element. In most cases, the interfering element is considered to be carbon since almost all organic compounds contain carbon. Carbon generates C_2 emissions and a continuum due to stray light over the complete spectrum. The continuum results in carbon interference at every point over the spectrum. The selectivity to carbon is improved since the emission wavelength at 221~222 nm is far separated from interfering carbon emission at 193.1 and 247.3 nm. Not only are there no significant carbon emission lines in this wavelength region, but the carbon continuum is reduced by preventing carbon deposition on the electrodes. The selectivity to carbon is over 1000, which is better than the other atomic emission detectors without a correction system (20 reported by McCormack et al. [22], 100 by McLean et al. [23], 610 by Estes et al. [24]). The selectivity to oxygen is also determined using CH_3OH and C_2H_5OH, and is found to be greater than 1500. The selectivity of the atomic emission detectors is greatly increased by using a triple-slit-exit system [25,26], or by using diode array detection with a sophisticated software correction system which corrects the background by subtracting carbon interference [27,28]. The selectivity of the Cl-PDED may be increased by using a monochromator with less stray light.

5.5. Solvent tolerance

Since the selectivity to carbon is ~1000, a hydrocarbon solvent will cause the greatest interference with the Cl-PDED. In Fig. 12a the solvent was pentane and one can note the greater tail of the solvent than with methanol, which was used in most of the other chromatograms. There appears to be no permanent effect of the hydrocarbon solvent on the performance of the Cl-PDED. The only requirement in using a hydrocarbon solvent is to have sufficient separation of the solvent from the chlorine-containing compounds.

5.6. Effect of a hydrocarbon matrix

With a selectivity of ~1000 towards carbon, a high hydrocarbon matrix in a sample would be expected to give a significant contribution to the background which would obscure the KrCl emission from the Cl-PDED. This is also illustrated in Fig. 12a when the carbon emission from 510 pg of C from *n*-C_7H_{16} is comparable to the KrCl emission from 0.6 pg Cl from $CHCl_3$. If greater selectivity to carbon were attained, the interference from the hydrocarbon matrix would be diminished.

5.7. Quenching

The effect of hydrocarbon quenching of the KrCl emission is addressed in the fourth paper in this series. The chlorine-containing compounds were added to a gasoline sample and the quenching effect of the hydrocarbon co-elution was evaluated. At these concentrations the quenching of the KrCl emission was ~3–10%.

6. Comparison of Cl-PDED with electron capture detector

The electron capture detector is the most sensitive and useful detector in environmental analyses [19,20,29]. However, its responses are not uniform with respect to the determination of chlorinated compounds [19,20,30]. Fig. 24a and b shows the determination of chlorinated compounds using the parallel Cl-PDED–pulsed discharge electron capture detectors (PDECD). The column exit split ratio of PDECD–Cl-PDED was 7:1 in favor of the PDECD. For compounds having high electron capture coefficients, such as carbon tetrachloride, the PDECD sensitivities are higher than with the Cl-PDED. However, for compounds having low electron cap-

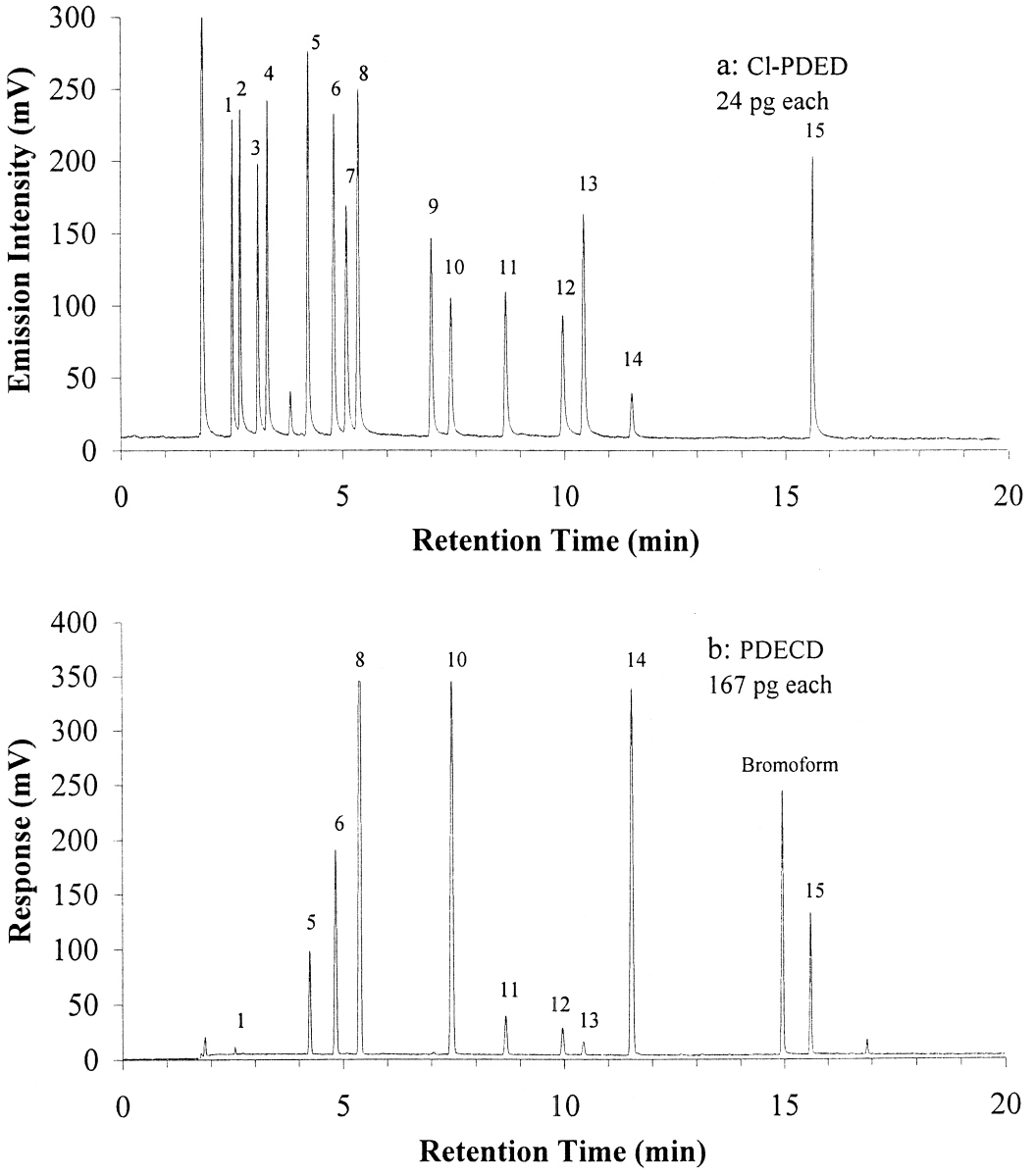

Fig. 24. Chromatograms of environmental protection agency (EPA) 502 mixture using parallel Cl-PDED–PDECD detectors. (a) Cl-PDED, (b) PDECD. Column: DB-5.625, 30 m×0.25 mm I.D., d_t: 0.5 μm, oven temperature program: 30°C (5 min), 5°C/min to 70°C, 20°C/min to 130°C (4 min), carrier gas: He, flow-rate: 30 cm/s, pulse width: 15 μs, pulse spacing: 400 μs, wavelength: 222.1 nm, detector gas: 0.2% krypton in helium, detector flow-rate: 3.5 ml/min, detector temperature: 150°C, injector temperature: 200°C, injector split ratio: 100:1, 0.2 μl sample in methanol. 1=1,1-Dichloroethene, 2=methylene chloride, 3=*trans*-1,2-dichloroethene, 4=1,1-dichloroethane, 5=chloroform, 6=1,1,1-trichloroethane, 7=1,2-dichloroethane, 8=carbon tetrachloride, 9=1,2-dichloropropane, 10=bromodichloromethane, 11=*cis*-1,3-dichloropropene, 12=*trans*-1,3-dichloropropene, 13=1,1,2-trichloroethane, 14=dibromochloromethane, 15=1,1,2,2-tetrachloroethane.

ture coefficients, such as methylene chloride, the PDECD responses are much lower than with the Cl-PDED, the Cl-PDED is a better choice to quantitatively analyze these chlorinated compounds. The peak tailing in the Cl-PDED is caused by the dead volume of a Tee at the inlet of the detector.

7. Conclusion

The Cl-PDED using ~0.2% Kr in helium as a reaction gas is the highest sensitive chlorine-selective detector. The advantages of the Cl-PDED, which are due to the use of KrCl* emission and a microvolume detector, can be briefly summarized as follows:

7.1. Advantages of using KrCl emission for the analysis of Cl*

1. The high sensitivity results from an ion–molecule reaction being 100–1000 times faster than a reaction of neutrals.
2. The emission of KrCl* in the UV region eliminates the need to purge the monochromator.
3. The improved selectivity results from the KrCl* emission wavelength at 221~222 nm, far separated from the C emissions at 193.1 and 247.3 nm.
4. The uniform response per Cl results from the reaction being sufficiently exothermic.

7.2. Advantages of the microvolume detector

1. The narrow discharge eliminates the entrance slit and accepts a larger fraction of the emitted radiation.
2. The microvolume of the pulsed discharge region results in high power/unit volume and leads to greater sensitivity.
3. The low detector flow-rate (~5 ml/min) reduces the helium gas consumption, which is important to the development of portable units.
4. The discharge electrodes are protected with a helium purge to prevent carbon deposition.
5. The inexpensive construction and the low consumption of gases and power make the Cl-PDED economically feasible.

There are four quantities commonly used to evaluate a selective detector, we would like to summarize them for the Cl-PDED as follows:

1. Sensitivity: a minimum detectability of 50 fg Cl/s has been observed.
2. Linearity: a linear range of over three orders of magnitude has been observed from an upper limit of ~150 pg down to the minimum detectability. The dynamic range is extended to four orders of magnitude.
3. Elemental responses: for the eight compounds consisting of aliphatic, alkene, cyclic and aromatic-chloro compounds the variation in response/pg Cl was less than ±5%. This variation should be representative of the response/pg Cl obtained for other chlorinated compounds.
4. Selectivity: the selectivity to carbon is about 1000. The limit of this selectivity is probably due principally to stray light in the monochromator. A double monochromator could be used which would diminish the stray light greatly to further improve the selectivity.

Acknowledgements

The authors would like to thank Dr. Edward C.M. Chen, Dr. Huamin Cai, Dr. Janardhan Madabushi, Mr. Max Loy and members of the detector group at Valco Instruments for their help in making the detector and helpful discussions on research. We would also like to thank the Robert A. Welch Foundation (Grant E-095) and Valco Instruments Co., Inc. for financial support on this project. We would like to express our appreciation to Valco Instruments Co., Inc. for providing the facilities for this project.

References

[1] R.C. Hall, J. Chromatogr. Sci. 12 (1974) 152.
[2] R.C. Hall, US Pat., 3 934 193, 1976.
[3] R.C. Hall, US Pat., 4 555 383, 1985.
[4] R.C. Hall, CRC Crit. Rev. Anal. Chem. 7 (1978) 323.
[5] R.C. Hall, in: H.H. Hill, D.G. McMinn (Eds.), Detectors For Capillary Chromatography, Wil, New York, 1992, p. 109, Chapter 6.
[6] M.L. Duffy, R.K. Simon Jr., L. Anderson, in: presented at Pittcon'97, Atlanta, 1997, Abstract 575.
[7] R.D. Snelling, M.L. Duffy, in: presented at Pittcon'98, New Orleans, 1998, Abstract 819.
[8] R.D. Snelling, in: presented at Pittcon'98, New Orleans, 1998, Abstract 820.
[9] M. Tsuji, M. Furusawa, H. Kouno, Y. Nishimura, J. Chem. Phys. 94 (1991) 429.
[10] M. Tsuji, T. Muraoka, H. Kouno, Y. Nishimura, J. Chem. Phys. 97 (1992) 1076.
[11] R.B. Jones, J.H. Schloss, J.G. Eden, J. Appl. Phys. 71 (1992) 1674.

[12] W.E. Wentworth, K. Sun, D. Zhang, J. Madabushi, S.D. Stearns, J. Chromatogr. A 872 (2000) 119.
[13] W.E. Wentworth, H. Cai, S.D. Stearns, J. Chromatogr. A 688 (1994) 135.
[14] W.E. Wentworth, H. Cai, J. Madabushi, Y. Qin, S.D. Stearns, C.J. Meyer, Process Contr. Qual. 5 (1993) 193.
[15] S.V. Vasin, W.E. Wentworth, S.D. Stearns, C.J. Meyer, Chromatographia 34 (1992) 226.
[16] W.E. Wentworth, Y. Qin, S. Wiedeman, S.D. Stearns, J. Madabushi, Applied Spectros. 49 (1995) 1282.
[17] A.N. Zaidel, E.Ya. Shreider, in: Vacuum Ultraviolet Spectroscopy, Ann Arbor–Humphrey Science Publishers, Ann Arbor, 1970, p. 13, translated by Z. Lerman.
[18] R.W.B. Pearse, A.G. Gaydon, in: The Identification of Molecular Spectra, Chapman and Hall, London, 1976, p. 86.
[19] W.E. Wentworth, Ela Desai D'Sa, H. Cai, J. Chromatogr. Sci. 30 (1992) 478.
[20] H. Cai, W.E. Wentworth, S.D. Stearns, Anal. Chem. 68 (1996) 1233.
[21] R.P.W. Scott, in: Introduction To Analytical Gas Chromatography, 2nd Edition, Marcel Dekker, New York, 1998, p. 172.
[22] A.J. McCormack, S.C. Tong, W.D. Cooke, Anal. Chem. 37 (1965) 1470.
[23] W.R. McLean, D.L. Stanton, G.E. Penketh, Analyst 98 (1973) 432.
[24] S.A. Estes, P.C. Uden, R.M. Barnes, Anal. Chem. 53 (1981) 1829.
[25] A. de Wit, J. Beens, in: E.R. Adlard (Ed.), Chromatography in the Petroleum Industry, Elsevier, Amsterdam, 1995, p. 159.
[26] A. de Wit, Spectrochim. Acta 38B (1983) 369.
[27] B.D. Quimby, J.J. Sullivan, Anal. Chem. 62 (1990) 1027.
[28] J.J. Sullivan, B.D. Quimby, Anal. Chem. 62 (1990) 1034.
[29] E.P. Grimsrud, in: H.H. Hill, D.G. McMinn (Eds.), Detectors For Capillary Chromatography, Wil, New York, 1992, p. 83, Chapter 5.
[30] W.E. Wentworth, Y. Wang, W. Odegard, E.C.M. Chen, S.D. Stearns, J. Chromatogr. Sci. 34 (1996) 368.